Cell. Mol. Life Sci. 66 (2009) 1741 – 1754
1420-682X/09/101741-14
DOI 10.1007/s00018-009-9181-8

Cellular and Molecular Life Sciences

Research Article

Sphingosine 1-phosphate induces differentiation of adipose tissue-derived mesenchymal stem cells towards smooth muscle cells

P. Nincheri[a], P. Luciani[b], R. Squecco[c, d], C. Donati[a, d], C. Bernacchioni[a, d], L. Borgognoni[e], G. Luciani[c], S. Benvenuti[b], F. Francini[c, d] and P. Bruni[a, d, *]

[a] Department of Biochemical Sciences, Viale G. B. Morgagni 50, University of Florence, 50134 Florence (Italy), Fax : +390554598905, e-mail: paola.bruni@unifi.it
[b] Endocrine Unit, Department of Clinical Physiopathology, Center for Research, Transfer and High Education on Chronic, Inflammatory, Degenerative, and Neoplastic Disorders (DENOThe), University of Florence, 50139 Florence (Italy)
[c] Department of Physiological Sciences, University of Florence, Firenze I-50134 (Italy)
[d] Interuniversity Institute of Myology, Viale G. B. Morgagni 50, University of Florence, 50134 Florence (Italy)
[e] Plastic Surgery Unit-Regional Melanoma Referral Center, Tuscan Tumor Institute (ITT), Santa Maria Annunziata Hospital, Florence (Italy)

Received 06 March 2009; accepted 17 March 2009
Online First 2 April 2009

Abstract. Sphingosine 1-phosphate (S1P) is a bioactive sphingolipid which regulates multiple biological parameters in a number of cell types, including stem cells. Here we report, for the first time, that S1P dose-dependently stimulates differentiation of adipose tissue-derived mesenchymal stem cells (ASMC) towards smooth muscle cells. Indeed, S1P not only induced the expression of smooth muscle cell-specific proteins such as α-smooth muscle actin (αSMA) and transgelin, but also profoundly affected ASMC morphology by enhancing cytoskeletal F-actin assembly, which incorporated αSMA. More importantly, S1P challenge was responsible for the functional appearance of Ca^{2+} currents, characteristic of differentiated excitable cells such as smooth muscle cells. By employing various agonists and antagonists to inhibit S1P receptor subtypes, $S1P_2$ turned out to be critical for the pro-differentiating effect of S1P, while $S1P_3$ appeared to play a secondary role. This study individuates an important role of S1P in AMSC which can be exploited to favour vascular regeneration.

Keywords. Sphingosine 1-phosphate, adipose tissue-derived mesenchymal stem cells, smooth muscle cells, cell differentiation.

Introduction

Adipose tissue-derived mesenchymal stem cells (AMSC), similar to mesenchymal stem cells isolated from bone marrow, exhibit immunomodulatory properties and differentiation potential towards diverse cell types such as adipogenic, osteogenic, chondrogenic, and myogenic lineages [1]. AMSC are a promising cell type because of their ease of isolation and expansion, their multipotency and their low immunogenicity [2]. However, in order to fully utilize

* Corresponding author.

the therapeutic potential of AMSC, it is important to understand their intrinsic properties and the role of the microenvironment in modulating their behaviour and function. Microenvironmental factors such as mechanical cues, soluble factors and matrix properties not only regulate AMSC differentiation, but also modulate AMSC signalling to the surrounding environment. Due to their ability to differentiate into smooth muscle cells (SMC), AMSC may be used for the formation of contractile layers in tissue-engineered vascular grafts. In addition, direct cell transplantation using AMSC is under investigation for treating cardiovascular disease such as myocardial ischemia. In this regard injected AMSC are known to be rapidly integrated into the regenerating tissue, differentiate into SMC, and promote neovascularisation [3, 4]. A major challenge in the employment of AMSC in regenerative medicine is to induce their differentiation towards a specific lineage and to ensure the maintenance of the desired phenotype. Therefore, the understanding of the pathways involved in myogenic differentiation of AMSC is of key importance in the design of experimental strategy aimed at improving their regenerative potential.

Sphingosine 1-phosphate (S1P) is a pleiotropic bioactive lipid capable of regulating many diverse biological processes mainly acting through a panel of five specific receptors, named S1P receptors (S1PR) ($S1P_{1-5}$) [5, 6]. S1P is abundant in plasma, where is largely bound to high density lipoproteins [7], but it can also act as local mediator, being synthesized and released by numerous cell types in response to a variety of stimuli. It is becoming increasingly clear that the expression pattern of S1PR is critical for the final effect elicited by the bioactive lipid in a given cell type, since individual receptor subtypes are coupled to different and even opposing signalling cascades, being consequently implicated in the regulation of biological responses in opposite fashion. Thus, S1P has been shown to elicit differential functional responses in SMC, including a robust pro-mitogenic action accompanied by induction of SMC differentiation marker genes [8, 9], Ca^{2+}-dependent contraction [10], and positive or negative regulation of cell migration [11–13], likely due to differences in the relative S1PR isoform expression in cultured SMC. The relevant functional role of S1P and its specific receptors in the development and maintenance of smooth muscle phenotype is highlighted by studies performed in mice genetically null for individual S1PR isoforms. In this regard $S1P_1$-null mice, which are embryonically lethal, exhibit impaired homing of SMC to developing blood vessels, suggesting that $S1P_1$ is critically implicated in vascular SMC migration *in vivo* [14]. However, the more severe and earlier vessel defects observed in the $S1P_1/S1P_2$ and $S1P_1/S1P_2/S1P_3$ triple null mouse embryos favour the concept that all these S1PR subtypes are required for the development of a stable and mature vascular system during embryonic development [15]. In view of the pivotal role played by S1P in the development of smooth muscle and in maintaining tissue plasticity, here we have investigated whether the bioactive lipid can have a role in the commitment to myogenic lineage of multipotent ASMC. Presented results demonstrate for the first time that S1P promotes differentiation of ASMC towards SMC, not only by enhancing the expression of myogenic marker proteins but also by inducing the onset of ionic currents which are characteristic of myogenic phenotype.

Materials and methods

Materials. Media and sera for cell cultures were purchased from Life-Technologies (Grand Island, NY) and tissue plastic-ware was obtained from Falcon (Oxnard, CA). Other cell culture reagents, biochemicals, TRIreagent, protease inhibitor cocktail, monoclonal anti-alpha smooth muscle actin (αSMA) antibodies, tetramethylrhodamine B isothiocyanate (TRITC)-phalloidin conjugate and bovine serum albumin (BSA) were purchased from Sigma (St. Louis, MO, USA). Secondary antibodies conjugated to horseradish peroxidase and non fat dry milk were obtained from Santa Cruz Biotechnology, Inc. (Santa Cruz, CA, USA). Monoclonal antibodies against β-actin was from Cytoskeleton Inc., (Denver, CO, USA). Goat anti-SM22-alpha/transgelin antibodies were from Everest Biotech (Oxfordshire, OX, U.K.). Enhanced chemiluminescence (ECL) reagents were obtained from GE Healthcare Europe GmbH (Milan, Italy). D-erythro-S1P and sphingosylphosphorylcholine (SPC), were purchased from Calbiochem, (San Diego, USA). Specific antagonists of S1PR, VPC23019 and JTE-013 were obtained from Tocris Cookson Ltd., (Bristol, U.K.). Fluorescein horse anti-mouse secondary antibody was obtained from Vector (Burlingame, CA, USA). Nucleospin®RNAII was from Macherey-Nagel (Duren, Germany). All reagents and probes required to perform real time PCR were from Applied Biosystems Inc., (Foster City, CA, USA).

Isolation, culture and characterization of AMSC. AMSC were obtained from human subcutaneous adipose tissue and cultured as described previously [16] with some modifications. Briefly, tissue was washed extensively with sterile phosphate-buffered saline (PBS) to remove contaminating debris and red

blood cells. Successively, tissue was minced and enzymatically dissociated using 0.35 % collagenase for 45 min at 37 °C under gentle agitation. The collagenase was inactivated with an equal volume of DMEM supplemented with 10 % fetal bovine serum (FBS), 100 u/ml penicillin, 100 μg/ml streptomycin and 1 μg/ml fungizone (growth medium) and the infranatant centrifuged for 10 min at 800 x g. Then supernatant was discarded and cellular pellet was resuspended in growth medium and filtered through a 150-μm mesh filter to remove debris. The filtrate was centrifuged as detailed above and plated onto tissue culture dish in growth medium.

Immunophenotyping and differentiation of AMSC. The morphologically homogeneous population of AMSC was analyzed for the expression of cell surface molecules using flow cytometry procedures. AMSC, recovered from flasks by trypsin-EDTA treatment and washed in Hanks' Balanced Salt Solution and 10 % FBS, were resuspended in CellWASH buffer (0.1 % sodium azide in PBS) with 2 % FBS. Aliquots ($1.5x10^5$ cells/100 μl) were incubated with the following conjugated monoclonal antibodies: CD34-PE, CD45-FITC, CD14-PE (in order to quantify hemopoietic-monocytic contamination); CD29-PE, CD44-FITC, CD166-PE, CD90-PE, CD73-PE, HLA-DP Q R, HLA-ABC and CD105-PE. Non-specific fluorescence and morphologic parameters of the cells were determined by incubation of the same cell aliquot with isotype-matched mouse monoclonal antibodies. Incubations were performed for 20 min and thereafter the cells were washed and resuspended in 100 μl of CellWASH; 7-amino-actinomycin D was added in order to exclude dead cells from the analysis. Flow cytometric acquisition was performed by collecting 10^4 events on a FACScan (argon laser equipped; Becton Dickinson) instrument and data were analyzed on DOT-PLOT bi-parametric diagrams using CELL QUEST software (Becton Dickinson, Franklin Lakes, NJ, USA) on Macintosh PC. The ability of AMSC to differentiate along osteogenic, adipogenic, and chondrogenic lineages was routinely assayed, as described previously by Pittenger et al. [17]. Osteogenic and chondrogenic differentiation were evaluated morphologically. Petri dishes were stained to assess glucosamynoglycans by Toluidine Blu and mineral-bound extracellular matrix by Alizarin Red-S. Adipogenic differentiation was evaluated by Sudan Black B stain; lipid droplets were photographed under light microscopy. For differentiation into smooth muscle, cells were seeded in six-well plates and when confluent were shifted to DMEM without serum containing 1 mg/ml BSA. To evaluate differentiation into smooth-muscle-like cells, AMSC were serum-starved for 24 h and challenged with the indicated concentration of S1P or SPC for the selected time-intervals.

RT-PCR. One μg of total RNA extracted with TriReagent from AMSC was reverse transcribed into DNA as previously described [18] and subjected to PCR using the following software-designed oligonucleotides: $S1P_1$ forward, 5'-CCTATCATGGGCTGGAACTGCATC-3'; $S1P_1$ reverse, 5'-CCCCAGAAAGACGAAGGG-GACAACCCAGAG-3'; $S1P_2$ forward, 5'TGCCGC-ATGCTTCTGCTCATCGGG-3'; $S1P_2$ reverse, 5'-CTGGAGGGCAACACGGTGGTCTGA-3'; $S1P_3$ forward, 5'-CTGCTCTACCATCCTGCCCCTCTAC-3'; $S1P_3$ reverse, 5'-GCACTTCAGAATGGGATCTT-CTGCAAC-3'; $S1P_4$ forward, 5'-AGCCTTCTGCC-CCTCTACTC-3'; $S1P_4$ reverse, 5'-GTAGATGATG-GGGTTGACCG-3'; $S1P_5$ forward, 5'-TACGTGCTC-TTCTGCGTG-3'; $S1P_5$ reverse, 5'-CCTGCAGGCC-GATCCCTTCCT-3'; β-actin forward, 5'-GCGGGA-AATCGTGCGTGACATT-3'; β-actin reverse, 5'-GA-TGGAGTTGAAGGTAGTTTCGTG-3'. PCR amplification products were separated on a 1.4 % agarose gel.

Quantitative real-time RT-PCR. The quantification of S1PR mRNA was performed by real-time RT-PCR based on TaqMan technologies. Total RNA to be subjected to reverse transcription was extracted from AMSC cells (basal conditions and after S1P treatment) using Nucleospin®RNAII (Macherey-Nagel Duren, Germany) with DNAse treatment according to the manufacturer's instructions, the concentration determined spectrophotometrically with Nanodrop® ND-1000. First strand cDNA was synthesized using "TaqMan Reverse transcription Reagents" (Applied Biosystems) with Reaction Buffer 1X; $MgCl_2$ 5.5 mM; dNTPs 2 mM; RNAse Inhibitor 1U; random hexamers 1.25 μM; MuLV 2U. PCR was carried out in triplicate on 20 ng cDNA, employing TaqMan Gene Expression Assays (Applied Biosystems) for $S1P_1$, $S1P_2$, $S1P_3$, $S1P_4$ and $S1P_5$. The mRNA quantitation was based on the comparative Ct method [19] and data were normalized to ribosomal 18S RNA expression.

Electrophysiological recordings. Whole-cell responses of AMSC adherent on glass coverslips were conventionally recorded in both voltage-clamp and current-clamp modes with pipettes of 3–7 MΩ resistance, filled with a solution containing: 150 mM CsBr, 5 mM $MgCl_2$, 10 mM EGTA and 10 mM HEPES. Coverslips with the adherent AMSC were superfused at a rate of 1.8 ml min^{-1} with a physiological bath solution: 150 mM NaCl, 5 mM KCl, 2.5 mM $CaCl_2$, 1 mM $MgCl_2$, 10 mM D-glucose and 10 mM HEPES. Alternatively, an external TEA-Ca^{2+} bath solution was used: 10 mM $CaCl_2$, 145 mM TEABr and

10 mM HEPES. This solution allowed us to have Ca^{2+} as the only permeant cation and, thus, to record only Ca^{2+} currents. In turn, 10 μM nifedipine was used to block L-type Ca^{2+} channels. pH was 7.4 and 7.2 for bath and pipette solution, respectively.

The technique, set up, and electronics are as described in detail in Benvenuti et al. [20]. Briefly, the pipettes were mounted on a hydraulic micromanipulator and connected to Axopatch 200A amplifier (Axon Instruments, Union City, CA). Voltage- and current-clamp protocol generation and data acquisition were controlled by using an output and an input of the A/D-D/A interfaces (Digidata 1200; Axon Instruments) and Pclamp 9 software (Axon Instruments). Cells were discarded when they exhibited resting current fluctuations greater than 10 % during the recording. Currents were low-pass filtered at 2 kHz with a Bessel filter. For the activation pulse protocol the cell was held at –90 mV and step pulses, 1 – 5 seconds, from -80 to 50 mV, were applied in 10 mV increments. Linear leak and capacitance currents were cancelled on-line using the P/4 procedure. Experiments were performed at 22 °C.

The steady-state ionic current activation was evaluated by the equation

$$I_a(V) = G_{\max}(V - V_{rev})/\{1+\exp[(V_a - V)/k_a]\}$$

(eqn. 1) where $G_{\max}$ is the maximal conductance for the I_a, V_{rev} is the apparent reversal potential, V_{a} is the potential eliciting the half-maximal current size, k_{a} is the steepness factors.

Resting potentials were recorded by switching to the current-clamp mode the 200 B amplifier. Electrode capacitance was compensated before disrupting the patch. The passive properties parameters were estimated as in previous work [21, 22]. Access resistance (R_{a}) was not compensated for monitoring membrane area. The area beneath the capacitive transient and the time constant of the transient's decay (τ) were used to calculate the cell linear capacitance (C_{m}) and R_{a} from $\tau = R_{\text{a}}C_{\text{m}}$. The measurement of membrane resistance (R_{m}) was corrected for R_{a} and was calculated from the steady-state membrane current (I_{m}) using the relation: $R_{\text{m}} = (\Delta V - I_{\text{m}}R_{\text{a}})/I_{\text{m}}$, where ΔV is the command voltage step amplitude. The ratio $1/R_{\text{m}}$, that is the membrane conductance G_{m}, was used as an index of the resting cell permeability. The exponential rise of the voltage step causes underestimation of C_{m}, particularly when leak conductance increases greatly, so C_{m} was corrected using the relation $C_{\text{m}} = \Delta Q(R_{\text{m}}+R_{\text{a}})/R_{\text{m}}\Delta V$, where ΔQ is the sum of the time integral of the current transient and $I_{\text{m}}\tau$ elicited by each voltage step. C_{m}, was used as an index of the cell surface area assuming that membrane-specific capacitance is constant at 1 pF/μm^2. In the text current densities (pA pF^{-1}), instead of current amplitudes, were used to compare data obtained in different cells to avoid fluctuations of current amplitudes due to different cell sizes. Data are expressed as mean ± SEM.

Western blot analysis. AMSC were lysed for 30 min at 4 °C in a buffer containing 50 mM Tris, pH 7.5, 120 mM NaCl, 1 mM EDTA, 6 mM EGTA, 15 mM $Na_4P_2O_7$, 20 mM NaF, 1 % Nonidet and protease inhibitor cocktail (1.04 mM AEBSF, 0.08 μM aprotinin, 0.02 mM leupeptin, 0.04 mM bestatin, 15 μM pepstatin A, 14 μM E-64) essentially as described [23]. To prepare total cell lysates, cell extracts were centrifuged for 15 min at 10 000 g at 4 °C. Proteins (20 μg) from lysates were resuspended in Laemmli's sodium dodecylsulfate- (SDS) sample buffer. Samples were subjected to SDS-polyacrylamide gel electrophoresis (SDS-PAGE) for 90 min at 100 mA, before transfer of proteins to PVDF membranes, which were incubated 1 h at room temperature with 20 mM Tris, pH 7.5, 150 mM NaCl containing 0.1 % Tween 20 and 5 % nonfat milk. After rinsing, membranes were incubated overnight with the antibodies at 4 °C and then with specific secondary antibodies for 1 h at room temperature. Bound antibodies were detected using ECL reagents. Densitometric analysis of the bands was performed using Imaging and Analysis Software by Bio-Rad (Quantity-One).

Immunostaining and fluorescence microscopy. AMSC were seeded on microscope slides, pre-coated with 2 % gelatine, and then challenged with 1 μM S1P (2 mM stock solution in dimethylsulfoxide) for six days. Cells were fixed in 2 % paraformaldehyde in PBS for 20 min, and permeabilized in 0.1 % Triton-PBS for 30 min. Cells were then blocked in 3 % BSA for 1 h and incubated with anti-αSMA antibody for 2 h and Cy3-conjugated anti-mouse secondary antibody for 1 h. To stain F-actin filaments, the specimen was incubated with TRITC-phalloidin for 40 min. Images were obtained using a Leica SP5 laser scanning confocal microscope with 40X objective.

Results

S1PR have been individuated in a number of different stem cells, including human and mouse embryonic stem cells [24–26], mesoangioblasts [27] and more importantly, bone marrow-derived MSC [28]. However, the expression of S1PR in AMSC has not been investigated so far. Here, at first, we examined whether S1PR were expressed in AMSC. Amplified fragments of ~563, 650, 553, and 339 base pairs, corresponding to $S1P_1$, $S1P_2$ $S1P_3$ $S1P_4$ $S1P_5$ respec-

tively, were detected by semi-quantitative PCR analysis (Fig. 1A). Quantitative analysis of S1PR expression performed by real time PCR revealed that the relative mRNA abundance was: $S1P_1 >> S1P_3 > S1P_2 > S1P_4 > S1P_5$ (Fig. 1B).

Taking into account the multipotency of these cells and the recognized ability of S1P to exert pleiotropic effects on smooth muscle, we studied whether S1P can affect AMSC phenotype, by promoting the onset of myogenic lineage. For this purpose, AMSC were incubated in the presence of 1 μM S1P for various time-intervals, ranging from 1 to 10 days and total cell lysates were then employed for Western blot analysis of contractile proteins recognized as smooth muscle expression markers, such as αSMA and transgelin. Results presented in Figure 2A clearly show that S1P induced a time-dependent increase of protein content of both myogenic markers which was already appreciable at 24 h of incubation and was further increased at more prolonged times of incubation. As shown in Figure 2B, the induction of differentiation of AMSC towards smooth muscle elicited by S1P was dose-dependent: after six days of treatment, S1P, at concentrations as low as 100 nM was capable to augment the expression of αSMA as well as that of transgelin with maximal efficacy at 1 μM.

The morphological change provoked by the bioactive sphingolipid was clearly appreciable by confocal immunofluorescent microscopic analysis of ASMC performed to reveal the state of assembly of their cytoskeleton. Indeed, cell incubation with 1 μM S1P for six days profoundly altered the organization of the actin cytoskeleton, giving rise to the formation of numerous stress fibers arranged in a web-like structure anchored to the plasma membrane, resulting from G-actin polymerization into F-actin filaments which were immunorevealed by TRITC-phalloidin (Fig. 3). The observed effect of S1P is in accordance with a number of previous reports in various cell types in which the sphingolipid was found to elicit cytoskeletal reorganization [29]. Most interestingly, the same figure shows that S1P treatment strongly induced the expression of αSMA, which was largely incorporated into actin stress fibers. In this regard, αSMA incorporation into F-actin filaments of AMSC is a characteristic feature of cell differentiation, which enables the cells to exert increased contractile activity.

Onset of SMC phenotype is characterized by the expression of specific ionic channels which account for the acquired ability to contract in response to membrane depolarization. Therefore we examined the electrophysiological properties of AMSC as well as their possible changes consequent to S1P challenge. The resting membrane potential evaluated by whole-cell patch clamp was -41.4 ± 3 mV. The passive properties, cell capacitance C_m and the normalized cell resting conductance G_m/C_m values were evaluated in voltage-clamp mode and were: 37.2 ± 2.5 pF and 1.5 ± 0.1 nS/pF (n = 78), respectively. The undifferentiated AMSC were then assessed for the functional expression of specific ionic channels. Electrophysiological analysis confirmed the mesenchymal nature of these cells, since in physiological bath solution they showed two kinds of outward K^+ currents: 1) a relatively slowly activating current, I_{Ks}, that occurred starting from -30 mV and was not- or slightly-inactivating at positive potentials during 4 s long pulses; mean current density was 53.7 ± 5.4 pA/pF at +50 mV (Fig. 4Aa and c); 2) a fast activating and non-inactivating current, I_{kr}, observed alone or coexisting with I_{Ks}, starting from -30 mV; mean current density

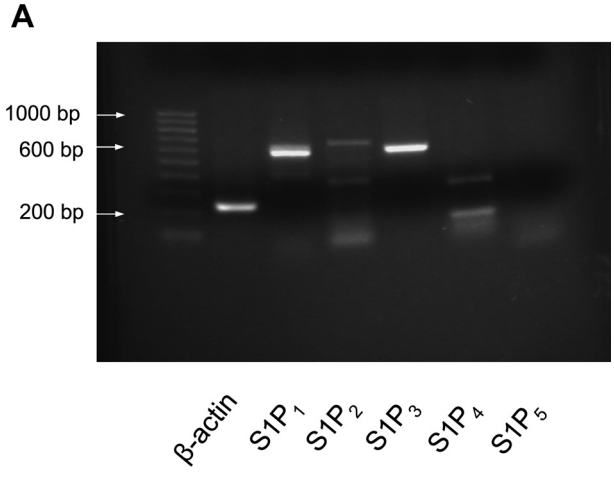

Figure 1. mRNA expression levels of S1PR in AMSC. (*A*) RT-PCR analysis of S1PR in AMSC using total cellular RNA. cDNAs corresponding to the expected length of $S1P_1$, $S1P_2$, $S1P_3$, $S1P_4$, were detected.

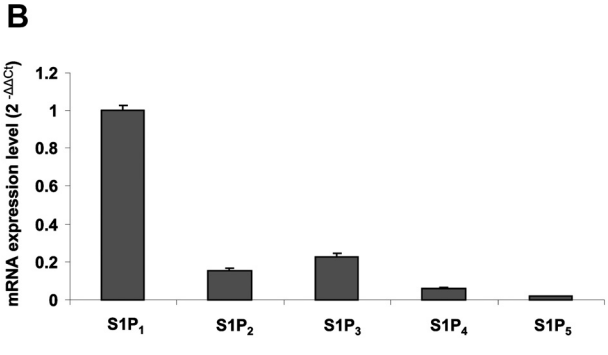

Figure 1. (*continued*) (*B*) Real time RT-PCR analysis. Quantitative mRNA analysis was performed by simultaneous amplification of the target $S1P_1$, $S1P_2$, $S1P_3$, $S1P_4$ and $S1P_5$ genes together with the housekeeping gene 18S rRNA. Results are expressed as fold changes according to the $2^{-\Delta\Delta CT}$ method, utilizing $S1P_1$ as calibrator. Data are from one representative experiment performed in triplicate and repeated three times with analogous results.

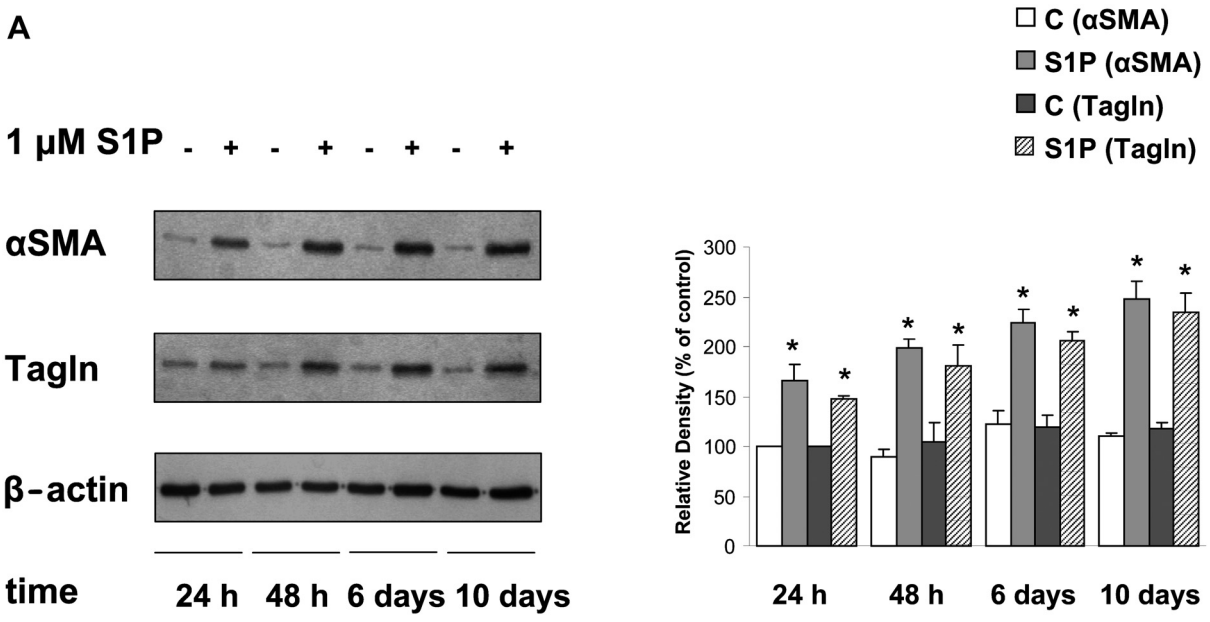

Figure 2. Effect of S1P on the differentiation of AMSC into smooth muscle-like cells. Time course (*A*) and dose-dependence (*B*) of the effect of S1P on the expression levels of smooth-muscle markers αSMA and transgelin (Tagln) analyzed by Western blot analysis. Confluent AMSC were incubated with DMEM containing 1 mg/ml BSA for the indicated period of time in the absence (-) or in the presence (+) of 1 μM S1P (*A*) or with the indicated concentrations of S1P for 6 days.

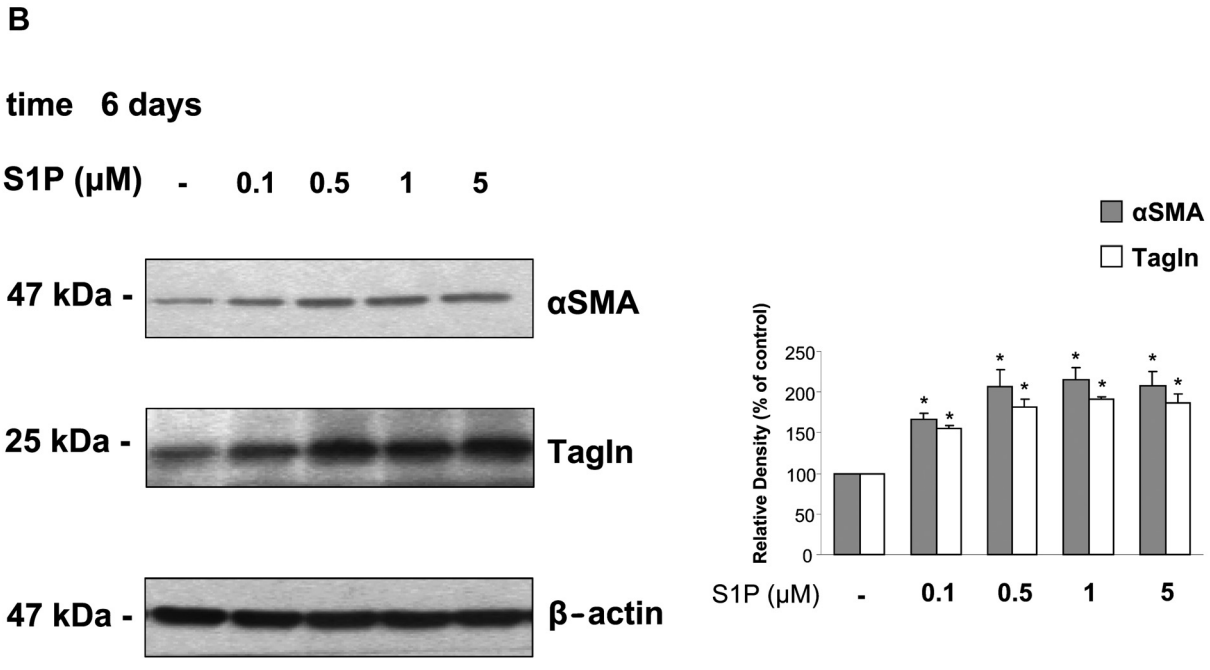

Figure 2. (*continued*) Right panels: The histograms represent mean densitometric quantification (n = 3) of αSMA and Tagln versus β-actin, reported as percentage relative to the intensity of the band corresponding to control (24 h) set as 100. The effect of S1P was statistically significant by Student's *t*-test, (*P < 0.05).

was 5.4 ± 1 pA/pF at +50 mV (Fig. 4Ab and c). Thus, the outward current recorded in control bath solution at a holding potential of -90 mV was due to at least two kinds of K^+ channels roughly corresponding to I_{Ks} and I_{Kr} described in human bone marrow-derived mesenchymal stem cells [30, 32] and in human embryonic stem cells [33]. These currents were absent when records were achieved in 20 mM-TEA or TEA–Ca^{2+} bath solution, confirming that they were K^+ currents. Moreover, in 20 mM-TEA bath solution Na^+ inward

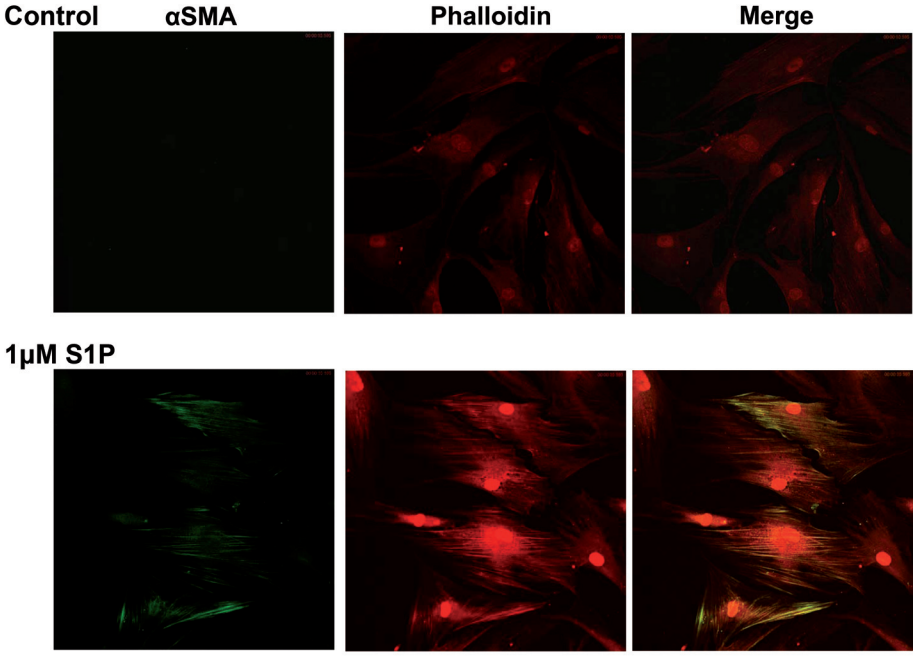

Figure 3. Effect of S1P on the levels and localization of αSMA in AMSC. Serum-starved AMSC were treated (+) or not (control) with 1 μM S1P for six days, immunostained with anti-αSMA and TRITC-phalloidin and analysed using Leica SP5 laser scanning confocal microscope with a 40X magnification. Images representative of three independent experiments are shown.

currents were never observed in any of the investigated cells whereas Ca^{2+}currents were rarely recorded (6 out of 78 cells).

AMSC which were incubated for 10 days in the presence of 1 μM S1P showed significant changes with respect to untreated cells, exhibiting a greater C_m and a smaller G_m/C_m (80.1 ± 4 pF, $P < 0.05$; 0.5 ± 0.05 nS/pF, $P < 0.05$; $n = 28$). Moreover, cells were more hyperpolarized since the resting membrane potential was -50.1 ± 3.3 mV ($P < 0.05$). The reduced G_m/C_m may explain the hyperpolarized state of the cell. The increased surface membrane, evaluated by the C_m parameter, suggested the occurrence of cell growth but the hyperpolarized state of the cell together with the reduced G_m/C_m strongly supports the evidence that the enhancement of cell surface is actually related to cell differentiation. This notion is further strengthened by recent studies performed in human fetal cardiomyocytes, in which it was found that cell hyperpolarization corresponds to a significant increase of their surface area and the appearance of inward Na^+ and Ca^{2+} currents, indicating that cells are differentiated towards excitable cardiomyocytes [33, 34]. In agreement, S1P-stimulated AMSC showed drastic differences also in the type of the elicited currents. Inward transient currents preceded outward K^+ currents in all the investigated cells (Fig. 4Ba). To evaluate the involvement of functional Na^+ and Ca^{2+} channels, we used 20 mM-TEA bath solution. A fast inward tetrodotoxin-sensitive Na^+ current was observed with small amplitude in some of the investigated cells (6 out of 28) (data not shown). Moreover, in all investigated cells inward transient current, $I_{Ca,T}$, was recorded from -50 mV with a peak at 80–100 ms. From -30 mV it was followed by a slower decay, suggesting the activation of L-type Ca^{2+} channels (Fig. 4Bb). This was confirmed by using nifedipine that blocks L-type but not T-type Ca^{2+} current (Fig. 4Bc). The Boltzmann parameters for these two current activations agree with T- and L-type Ca^{2+} current (Fig. 4Bb and c). I–V relations are shown in Figure 4Bd, where both the total Ca^{2+} current ($I_{Ca,tot}$) and the single T- ($I_{Ca,T}$) and L-type ($I_{Ca,L}$) components are depicted. Since the inward Na^+ and Ca^{2+} currents were not observed in undifferentiated cells or only in a low percentage [20, 22, 30–33], the strong increase in the number of cells eliciting I_{Na} (from less than 5 % up to 30 %) and the ability of all the cells to elicit I_{Ca} agree with an increasing expression of functional Na^+ and Ca^{2+} channels and suggests a differentiation towards a mature excitable cell phenotype.

In conclusion, the expression of Ca^{2+} currents with time course, size and kinetics similar to those reported in SMC of human bladder [34] confirms the differentiation state towards smooth muscle phenotype of S1P-simulated AMSC.

Individual S1PR subtypes have been found to be implicated in regulating multiple biological events in SMC. To ascertain whether one or more S1PR subtypes could account for the observed promyogenic

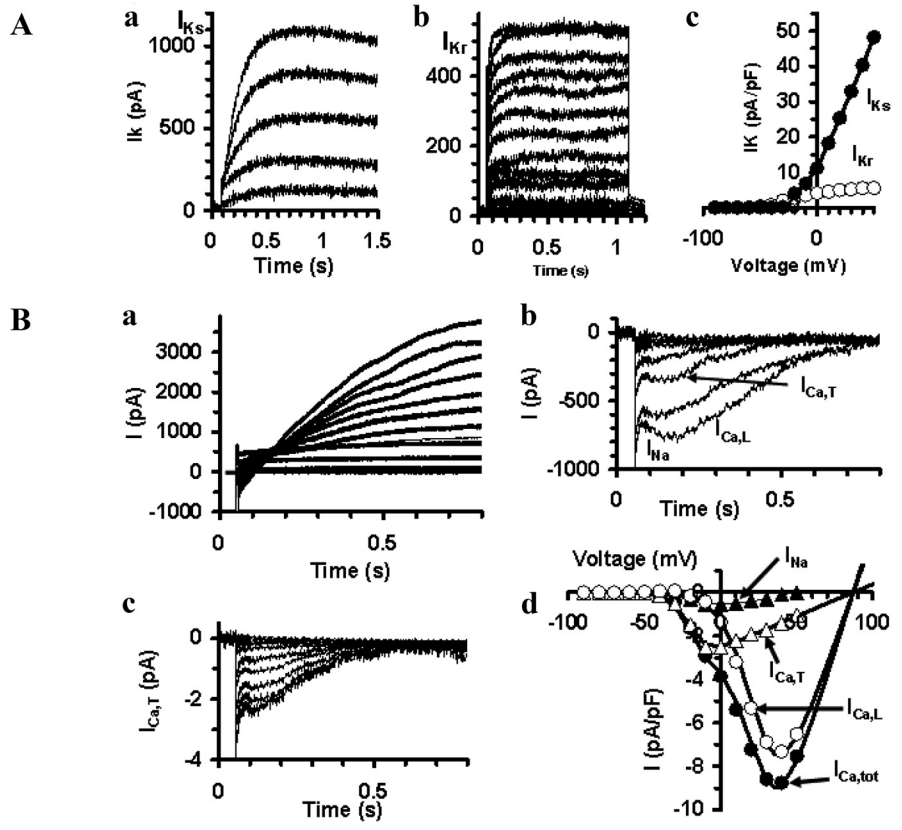

Figure 4. Effect of S1P on ionic currents in AMSC. (*A*) K^+ currents in AMSC. Original current traces, recorded in control (physiological) solution at a holding potential of -90 mV (voltage steps from -80 to 50 mV in 10-mV increments), showed a prevalent I_{Ks} (a) and a prevalent I_{Kr} (b). Related normalized I–V curves of I_{Ks} (filled circles) and I_{Kr} (open circles) (c). (*B*) Ca^{2+} currents in S1P-stimulated AMSC. In physiological bath solution inward currents precede outward K^+ currents (a). Na^+ (I_{Na}), T-type ($I_{Ca,T}$) and L-type Ca^{2+} ($I_{Ca,L}$) currents were recorded in the same cell in 20 mM-TEA bath solution before (4Bb) and after (4Bc), the addition of nifedipine. Related normalized I-V curves (d); $I_{Ca,L}$ was determined by subtracting $I_{Ca,T}$ from the total Ca^{2+} current ($I_{Ca,tot}$). The Boltzmann parameters, expressed as mean ± SEM, were for $I_{Ca,T}$: Va = -20 ± 4 mV, ka = 6.6 ± 2 mV and Vrev = 85 ± 15 mV; for $I_{Ca,L}$: Va = 20 ± 6 mV, ka = 10 ± 2 mV and Vrev = 87 ± 14 mV, and for INa: Va = -20 ± 4 mV, ka = 6.7 ± 2 mV and Vrev = 47 ± 5 mV.

effect elicited by S1P in AMSC, the effect of S1P was next examined in the presence of selective antagonists. Data reported in Figure 5A show that cell treatment with the $S1P_1$/$S1P_3$ antagonist VPC23019 (1 μM) resulted in an increased basal expression of both myogenic markers and into a slight decrease of the stimulatory effect exerted by S1P, while pharmacological inhibition of $S1P_2$ using JTE013 (1 μM), abrogated the S1P-induced enhancement of αSMA as well as that of transgelin. To exclude any possible involvement of $S1P_1$ in the pro-differentiating action exerted by S1P, AMSC were treated with 30 μM SEW2871, a selective $S1P_1$ agonist, and expression of myogenic markers evaluated after six days. Data reported in Figure 5B, show that the compound was unable to affect αSMA or transgelin content, strongly supporting the view that $S1P_1$ was disengaged from the pro-myogenic effect exerted by S1P. In keeping with this, the S1P-induced increase of αSMA or transgelin content was not affected by AMSC incubation with the selective $S1P_1$ antagonist W146 (10 μM) 30 min prior cell challenge, reinforcing the notion that $S1P_1$ is not implicated in S1P-directed expression of smooth muscle cell markers in AMSC.

The effect of S1PR antagonists on the S1P-induced appearance of Ca^{2+} currents was then investigated. To this end, initially we examined whether S1PR antagonists affect ASMC. ASMC pretreated with 1 μM JTE013 or 1 μM VPC23019, showed some changes with respect to control ASMC. The C_m values were similar (40 ± 3 and 45 ± 3, respectively), but G_m/C_m were decreased (1.1 ± 0.1, $P < 0.05$, and 1.2 ± 0.1, $P < 0.05$), whereas resting membrane potential was similar in JTE013-treated cells but was depolarized in VPC23019-treated cells (-40 ± 3 and -28 ± 2, $P < 0.05$, mV) (Fig. 6A–C). Notably, these cells did not show Na^+ currents, whereas there was a significant reduction of L-type Ca^{2+} current, I_{Kr} and I_{Ks} size (Fig. 6D and E). These results are compatible with blockade by these compounds of signalling brought about by S1P endogenously synthesized by AMSC. Next, it was assessed whether S1PR antagonists could affect S1P-induced electrophysiological properties by estimating the appearance of ionic currents typical of the excitable cells, focusing our attention on calcium currents for the relevant role they play in muscle physiology. ASMC pretreated with 1 μM JTE013 or 1 μM VPC23019 before 10-day treatment with 1 μM S1P showed a clear-cut impairment of S1P action on inducing differentiation towards SMC phenotype. With respect to S1P-stimulated cells, the hyperpolarized state was reduced (Fig. 6A), the membrane

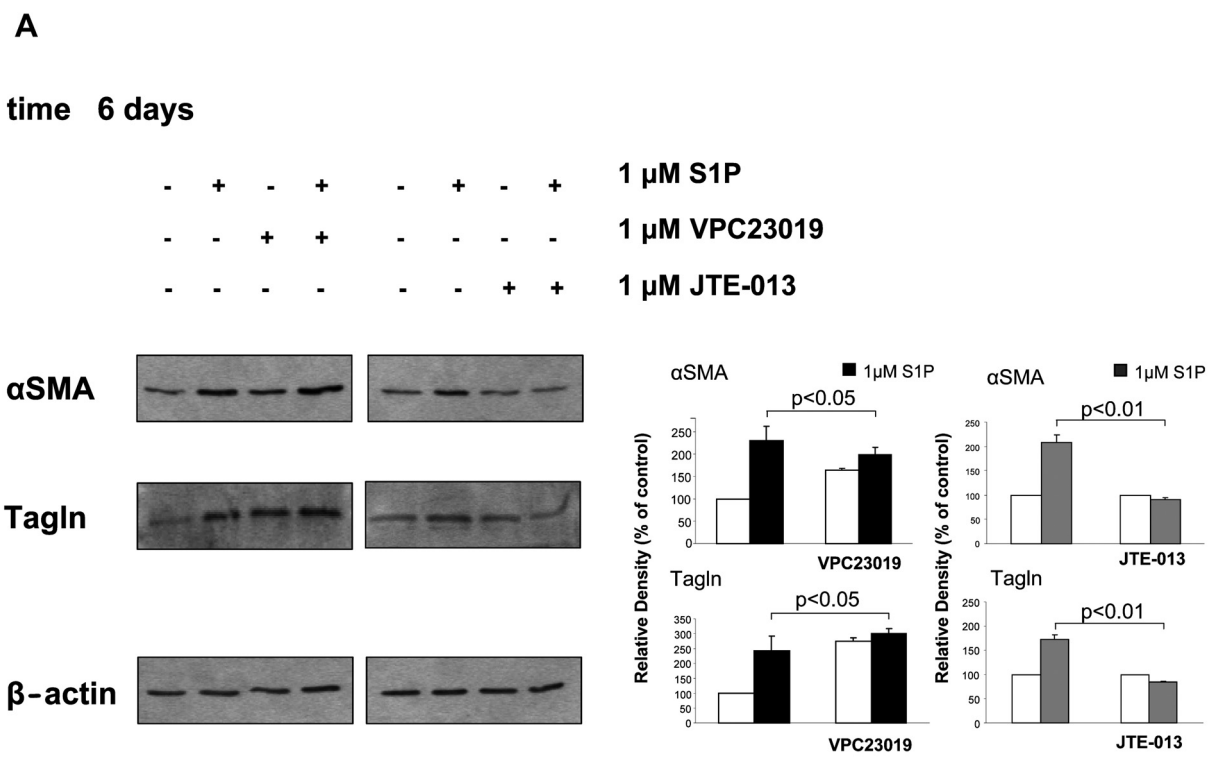

Figure 5. Role of S1PR in the effect of S1P on smooth muscle marker expression in AMSC. (*A*) Confluent AMSC were pretreated with 1 μM VPC23019 or 1 μM JTE-013 before being stimulated (+) or not (-) with 1 μM S1P for six days. The content of αSMA and transgelin (Tagln) was analyzed by Western blot of cell lysates. A blot representative of three independent experiments is shown. Right panel: the histograms represent mean densitometric quantification (n = 3) of αSMA and Tagln versus β-actin, reported as percentage relative to the intensity of the band corresponding to control set as 100. Statistical significance was calculated by Student's *t* test.

surface increase was blocked, given that C_m unchanged in value (Fig. 6B), the G_m/C_m diminished (Fig. 6C). Moreover, AMSC showed significant impairment of ionic currents. In particular, the drop of the I_{Ks} (Fig. 6D) and the increase in size of T- and L-type Ca^{2+} currents (Fig. 6E) were impaired. The comparison between JTE013 and VPC23019 treatment evidenced that although VPC23019 was effective, JTE013 determined a more significant impairment of S1P action on membrane potential, G_m/C_m, I_{Ks} and L-type Ca^{2+} current with respect to VPC23019.

Among the multiple cues capable of inducing AMSC differentiation towards smooth muscle-like cells, the sphingolipid SPC has recently received considerable attention [35, 36]. To better understand the relevance of the pro-differentiating action exerted by S1P in AMSC, the expression of smooth muscle markers in response to SPC was evaluated in comparison to S1P. As shown in Figure 7, SPC provoked a sustained increase in αSMA content which was already maximal at 1 μM, while it exerted a dose-dependent effect on transgelin with a maximum at 5 μM. Due to the comparable effects exerted by the two sphingolipids and the well-defined pro-myogenic effect of SPC, these data corroborate the notion that S1P is a potent inducer of smooth muscle phenotype.

Discussion

This study demonstrates for the first time that S1P is capable of triggering in AMSC the differentiation program responsible for switching towards smooth muscle-like cells. This conclusion is supported by multiple experimental evidence based on biochemical, cellular and physiological parameter evaluation. Indeed, incubation of AMSC with S1P was found to time-dependently enhance the protein content of two smooth muscle marker proteins such as αSMA and transgelin in a concentration-dependent fashion. Moreover, by immunofluorescence confocal microscopic analysis, it was evidenced that S1P stimulated actin stress fiber formation, and that the enhanced αSMA resulted specifically localized within F-actin filaments, in keeping with the increased contractile properties of differentiated phenotype. Importantly, S1P challenge also promoted the functional expression of Ca^{2+} ionic channels, which are specifically

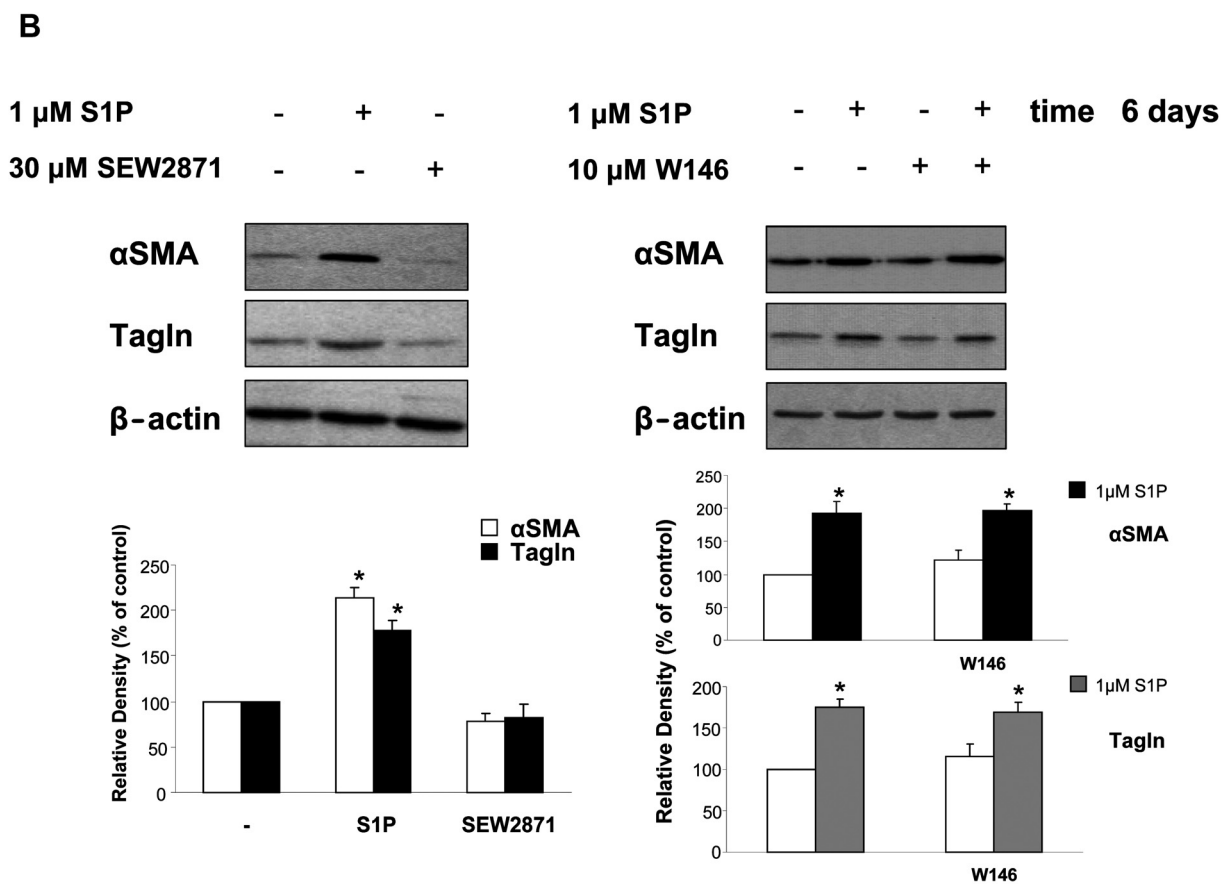

Figure 5. (*continued*) (*B*) Confluent AMSC were incubated with 30 μM SEW2871 or pretreated with 10 μM W146 before being stimulated (+) or not (-) with 1 μM S1P for six days. Levels of αSMA and transgelin (Tagln) expression were evaluated by Western blotting. A blot representative of three independent experiments is shown. Lower panels: The histograms represent mean densitometric quantification (n=3) of αSMA and Tagln versus β-actin, reported as percentage relative to the intensity of the band corresponding to control set as 100. Statistical significance was calculated by Student's *t* test.

implicated in the regulation of the contraction of SMC.

Notably AMSC, which exhibit exclusively K^+ currents characteristic of stem cells [20, 21, 30–32], upon challenge with S1P for 10 days, display not only an increased C_m, index of enhanced cell surface, a decrease of the specific membrane conductance and an hyperpolarized membrane potential, all hallmarks of cell differentiation [33], but also the onset of two distinct Ca^{2+} currents, namely L-type and T-type, which are a distinguishing feature of SMC. Indeed, the recorded currents in S1P-treated AMSC are reminiscent of those described in SMC of human bladder [34]. Thus, S1P not only induces the expression of proteins characteristic of smooth muscle-like cell phenotype, but importantly, gives rise to specific electrophysiological properties that render these cells capable of functioning *in vivo* as SMC.

In contrast with the present results, in a previous study aimed at characterizing the pro-myogenic properties of the sphingolipid SPC in AMSC, S1P was reported to be unable to affect αSMA expression, ruling out its involvement in differentiation towards SMC [35]. The investigation of the biological effects promoted by S1P in AMSC detailed here, carried out by employing multiple methodological approaches, is instead in favour of a key role of S1P in the commitment to myogenic lineage of these multipotent stem cells.

A multitude of different studies have shown that S1P exerts many diverse biological effects on a large variety of cell types, including the regulation of cell proliferation, differentiation and survival. Interestingly, stem cells have been recently shown to be responsive to S1P (reviewed in Pebay et al. [37]). Human embryonic stem cells are maintained in undifferentiated state by S1P treatment [26, 37], moreover the bioactive sphingolipid enhances their proliferation and exerts relevant pro-survival action 26, 38]. In agreement, S1P acts as a powerful mitogenic anti-apoptogenic cue in skeletal muscle progenitor cells named mesoangioblasts [27]. Addi-

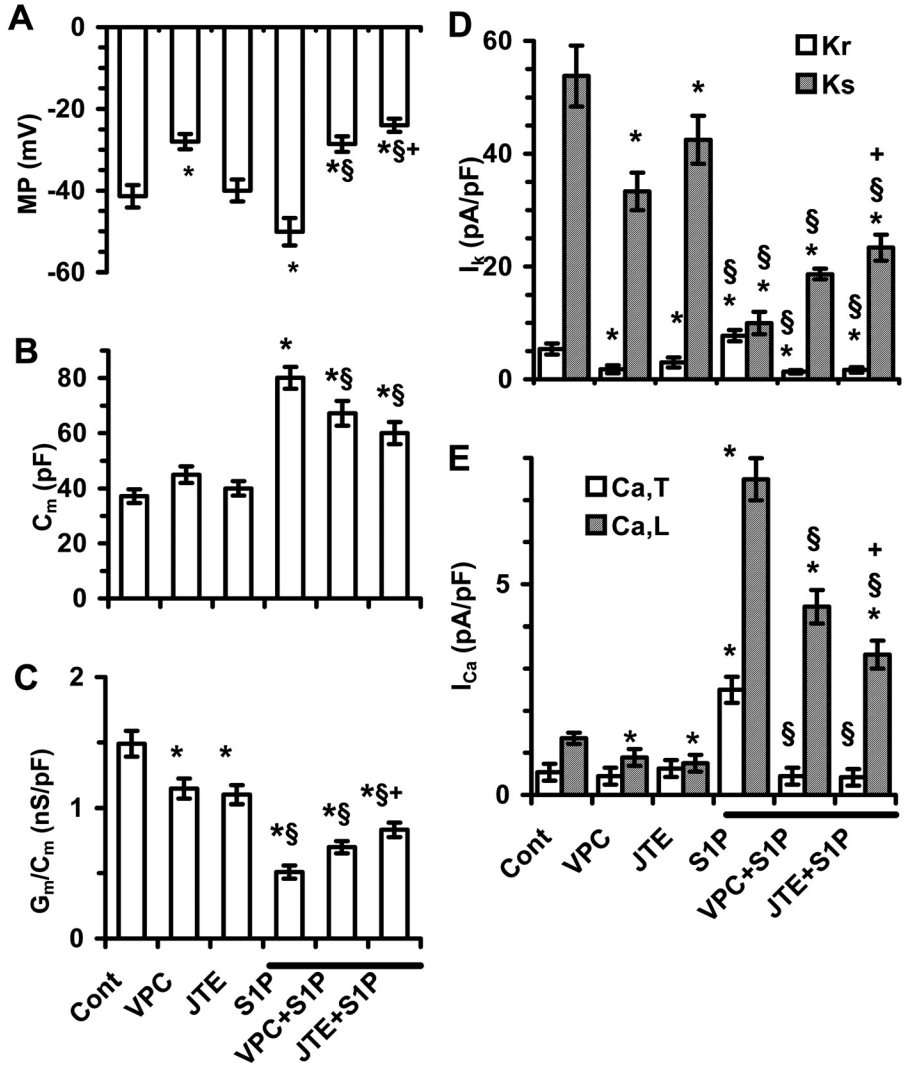

Figure 6. Effect of S1PR antagonists on electrophysiological parameters regulated by S1P in AMSC. The effect of pre-treatment with 1 μM VPC23019 (VPC) or 1 μM JTE013 (JTE) on 1 μM S1P action on resting membrane potential (*A*), membrane surface area (*B*), resting membrane conductance (*C*) and K^+ (*D*) and Ca^{2+} (*E*) currents was evaluated in AMSC. Data are expressed as mean ± SEM. Statistical significance evaluated by Anova test ($P < 0.05$) is indicated by * when referred to control, by § when referred to S1P stimulation, and by + when the effect of JTE013 was compared to that of VPC23019.

tionally, although the effect of S1P on undifferentiated mouse embryonic stem cells has not been described so far, cardiac differentiation is induced by S1P in embryoid bodies derived from mouse embryonic stem cells [39], supporting the view that S1P can exert multiple biological actions in stem cells. The here reported S1P ability of inducing smooth muscle differentiation of AMSC further strengthens the notion that S1P is a pleiotropic regulator of stem cells. Another notable finding of this study is that although ASMC bear a panel of five different S1PR subtypes ($S1P_{1-5}$), $S1P_2$ appears to be, by pharmacological inhibition, the most important for transmitting the myogenic signal brought about by S1P, with a secondary role played by $S1P_3$. Indeed, inhibition of $S1P_2$ by JTE-013 abrogated the induction of expression of myogenic markers and strongly reduced L-type Ca^{2+} currents as well as the appearance of the specific Ca^{2+} currents, whereas treatment with VPC23019 only attenuated the multiple biological effects elicited by S1P. Instead, on the basis of the effects exerted by a specific agonist, SEW2871, and a specific antagonist, W146, $S1P_1$, which is the most represented S1PR, at least at the mRNA level, does not appear to be implicated in transmitting the pro-differentiating action of S1P. In accordance with these findings, previously $S1P_2$ was identified as a key element in the modulation of SMC phenotype, being capable of selectively stimulating SMC differentiation in response to acute balloon injury [9]. The here observed partial overlapping function between $S1P_2$ and $S1P_3$ is in keeping with a redundant signalling through these receptors demonstrated in mice, where the respective encoding genes have been individually or simultaneously knocked-down [40, 41].

Although $S1P_2$ turned out to be clearly implicated in the S1P-dependent appearance of functional calcium currents and of key smooth muscle marker proteins, the $S1P_2$-mRNA of AMSC was largely less abundant than that of $S1P_3$ and $S1P_1$. This apparent incoherence

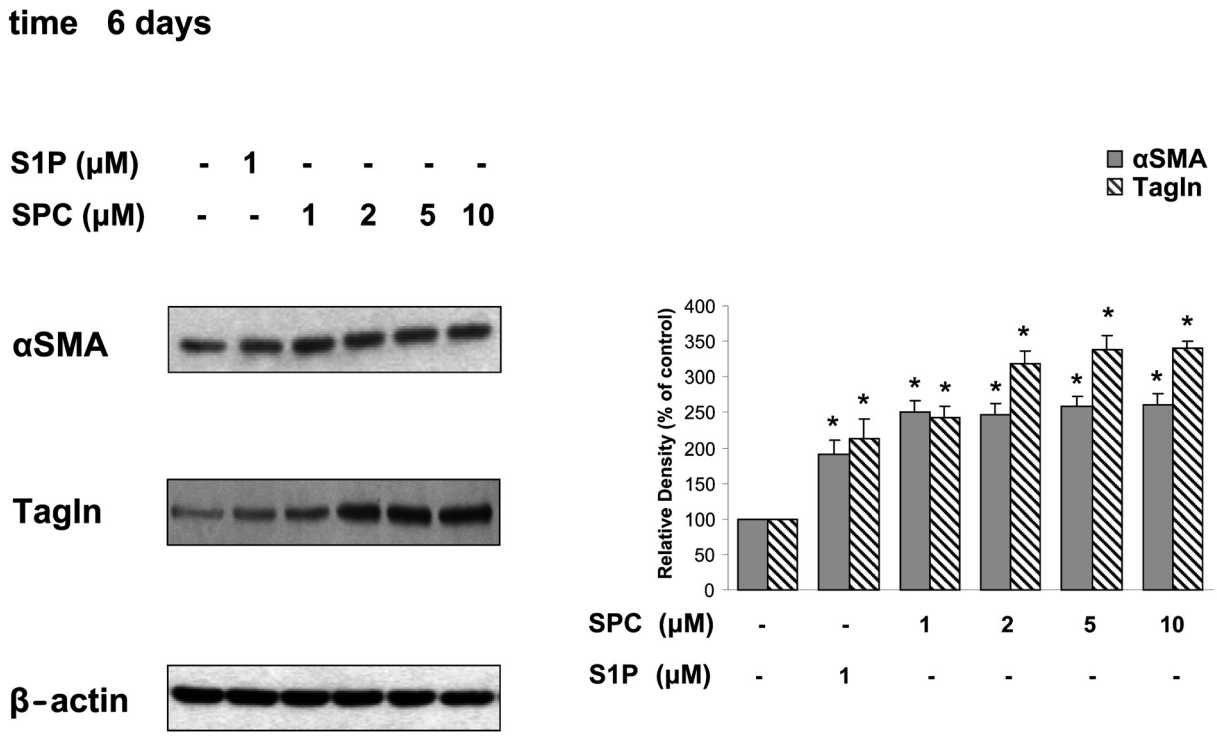

Figure 7. Comparison between S1P and SPC effect on smooth muscle-like differentiation of AMSC. The effect of 1 μM S1P and the indicated concentration of SPC on αSMA and transgelin (Tagln) expression were evaluated by Western analysis. AMSC were incubated in DMEM containing 1 mg/ml BSA for six days in the presence or in the absence of 1 μM S1P or of the indicated concentrations of SPC. Smooth muscle markers level was analyzed by Western blot. A blot representative of three independent experiments is shown. Right panel: The histograms represent mean densitometric quantification (n = 3) of αSMA and Tagln versus β-actin, reported as percentage relative to the intensity of the band corresponding to control set as 100. Asterisk indicates a statistically significant effect by Student's *t*-test ($P < 0.05$).

could be due to a complex regulation of S1PR subtype expression, in which mRNA levels do not reflect actual protein content; however, this hypothesis cannot be verified at the moment, given the lack of reliable antibodies specific for S1PR isoforms. An alternative explanation is that $S1P_2$ could be localized in functional domains of the plasma membrane favourable to its signalling, whereas others receptor subtypes were maintained in inactive signalling platforms. In this scenario, the actual functional coupling of S1PR could also depend on their dimeric state [42]. Interestingly, despite its reduced abundance, at least at the mRNA level, $S1P_2$ has a prominent role in other cell systems such as in myogenic differentiation of myoblasts [23], in the mitogenic response of mesoangioblasts [27] as well as in the inhibition of keratinocyte proliferation [43]. It will therefore be attractive to explore this issue as soon as adequate tools will become available.

The myogenic potential exerted by S1P in AMSC appears to be comparable to that of SPC, a structurally related sphingolipid whose pro-differentiating activity has been extensively investigated [35, 36]. In this regard, since the actual receptor(s) implicated in SPC action in AMSC has (have) not been identified so far and these stem cells lack SPC-specific receptors [44], it is tempting to speculate that SPC could act through S1PR, and particularly $S1P_2$, which exhibits affinity towards SPC one order of magnitude lower than S1P [45].

It has been clearly established that TGFβ is a central player in the differentiation process of AMSC towards smooth muscle [46, 47]. In this respect, it has been shown that SPC triggers the myogenic differentiation program through a TGFβ-dependent mechanism, being capable of stimulating the autocrine secretion of TGFβ [35]. Intriguingly, S1P is known to participate in a complex signalling interplay with TGFβ, which includes the transactivation of the TGFβ receptor and the subsequent activation of Smad3 by S1P, which accounts for the TGFβ-mimicking action of the sphingolipid [48], but also the TGFβ-dependent transcriptional regulation of sphingosine kinase which, by enhancing intracellular S1P content, accounts for key biological responses of TGFβ such as induction of fibrosis and protection from apoptosis [49, 50]. The here reported novel effect of S1P, which acts as an inducer of the myogenic program of AMSC, confirms the occurrence of overlapping functions between the two extracellular cues and suggests the hypothesis that

S1P metabolism participates into the mechanism by which TGFβ induces differentiation of AMSC into SMC.

Finally, recalling that S1P has been so far regarded as a pharmacological tool capable of maintaining the stemness of various types of stem cells, the present study strongly suggests that the biological actions of S1P in stem cells require deeper investigation, since further support has been provided to the concept that S1P is a multifunctional molecule which, possibly depending on the stem cell lineage, can not only maintain their stemness, but also induce cell differentiation. Both these effects are important but are obviously required at different stages of the stem cell manipulation used in regenerative medicine. These multifunctional properties of S1P must be taken into consideration before including this sphingolipid among the molecular tools beneficial for successful cell therapy.

Acknowledgements. This work was supported in part by funds from the University of Florence and Fondazione Cassa di Risparmio di Lucca to P.B.

1 Chamberlain, G., Fox, J., Ashton, B., Middleton, J. (2007) Concise review: mesenchymal stem cells: their phenotype, differentiation capacity, immunological features, and potential for homing. Stem Cells 25, 2739–2749
2 Noel, D., Djouad, F., Bouffi, C., Mrugala, D., Jorgensen, C. (2007) Multipotent mesenchymal stromal cells and immune tolerance. Leuk. Lymphoma 48, 1283–1289
3 Silva, G. V., Litovsky, S., Assad, J. A. R., Sousa, A. L. S., Martin, B. J., Vela, D., Coulter, S. C., Lin, J., Ober, J., Vaughn, W. K., Branco, R. V. C., Oliveira, E. M., He, R. M., Geng, Y. J., Willerson, J. T., Perin, E. C. (2005) Mesenchymal stem cells differentiate into an endothelial phenotype, enhance vascular density, and improve heart function in a canine chronic ischemia model. Circulation 111, 150–156
4 Yoon, Y. S., Wecker, A., Heyd, L., Park, J. S., Tkebuchava, T., Kusano, K., Hanley, A., Scadova, H., Qin, G., Cha, D. H., Johnson, K. L., Aikawa, R., Asahara, T., Losordo, D. W. (2005) Clonally expanded novel multipotent stem cells from human bone marrow regenerate myocardium after myocardial infarction. J. Clin. Invest 115, 326–338
5 Ishii, I., Ye, X., Friedman, B., Kawamura, S., Contos, J. J., Kingsbury, M. A., Yang, A. H., Zhang, G., Brown, J. H., Chun, J. (2002) Marked perinatal lethality and cellular signaling deficits in mice null for the two sphingosine 1-phosphate (S1P) receptors, S1P(2)/LP(B2)/EDG-5 and S1P(3)/LP(B3)/EDG-3. J. Biol. Chem. 277, 25152–25159
6 Pyne, S., Pyne, N. J. (2000) Sphingosine 1-phosphate signalling in mammalian cells. Biochem J 349, 385–402
7 Okajima, F. (2002) Plasma lipoproteins behave as carriers of extracellular sphingosine 1-phosphate: is this an atherogenic mediator or an anti-atherogenic mediator? Biochim. Biophys. Acta 1582, 132–137
8 Lockman, K., Hinson, J. S., Medlin, M. D., Morris, D., Taylor, J. M., Mack, C. P. (2004) Sphingosine 1-phosphate stimulates smooth muscle cell differentiation and proliferation by activating separate serum response factor co-factors. J. Biol. Chem. 279, 42422–42430
9 Wamhoff, B. R., Lynch, K. R., Macdonald, T. L., Owens, G. K. (2008) Sphingosine-1-phosphate receptor subtypes differentially regulate smooth muscle cell phenotype. Arteriosclerosis Thrombosis and Vascular Biology 28, 1454–1461
10 Rosenfeldt, H. M., Amrani, Y., Watterson, K. R., Murthy, K. S., Panettieri, R. A., Jr., Spiegel, S. (2003) Sphingosine-1-phosphate stimulates contraction of human airway smooth muscle cells. FASEB J. 17, 1789–1799
11 Kluk, M. J., Hla, T. (2001) Role of the sphingosine 1-phosphate receptor EDG-1 in vascular smooth muscle cell proliferation and migration. Circ. Res. 89, 496–502
12 Ryu, Y., Takuwa, N., Sugimoto, N., Sakurada, S., Usui, S., Okamoto, H., Matsui, O., Takuwa, Y. (2002) Sphingosine-1-phosphate, a platelet-derived lysophospholipid mediator, negatively regulates cellular Rac activity and cell migration in vascular smooth muscle cells. Circ. Res. 90, 325–332
13 Xu, S. Z., Muraki, K., Zeng, F., Li, J., Sukumar, P., Shah, S., Dedman, A. M., Flemming, P. K., McHugh, D., Naylor, J., Cheong, A., Bateson, A. N., Munsch, C. M., Porter, K. E., Beech, D. J. (2006) A sphingosine-1-phosphate-activated calcium channel controlling vascular smooth muscle cell motility. Circ. Res. 98, 1381–1389
14 Liu, Y., Wada, R., Yamashita, T., Mi, Y., Deng, C. X., Hobson, J. P., Rosenfeldt, H. M., Nava, V. E., Chae, S. S., Lee, M. J., Liu, C. H., Hla, T., Spiegel, S., Proia, R. L. (2000) Edg-1, the G protein-coupled receptor for sphingosine-1-phosphate, is essential for vascular maturation. J. Clin. Invest 106, 951–961
15 Kono, M., Mi, Y., Liu, Y., Sasaki, T., Allende, M. L., Wu, Y. P., Yamashita, T., Proia, R. L. (2004) The sphingosine-1-phosphate receptors S1P1, S1P2, and S1P3 function coordinately during embryonic angiogenesis. J. Biol. Chem. 279, 29367–29373
16 Zuk, P. A., Zhu, M., Ashjian, P., De Ugarte, D. A., Huang, J. I., Mizuno, H., Alfonso, Z. C., Fraser, J. K., Benhaim, P., Hedrick, M. H. (2002) Human adipose tissue is a source of multipotent stem cells. Mol. Biol. Cell 13, 4279–4295
17 Pittenger, M. F., Mackay, A. M., Beck, S. C., Jaiswal, R. K., Douglas, R., Mosca, J. D., Moorman, M. A., Simonetti, D. W., Craig, S., Marshak, D. R. (1999) Multilineage potential of adult human mesenchymal stem cells. Science 284, 143–147
18 Meacci, E., Vasta, V., Donati, C., Farnararo, M., Bruni, P. (1999) Receptor-mediated activation of phospholipase D by sphingosine 1-phosphate in skeletal muscle C2C12 cells. A role for protein kinase C. FEBS Lett. 457, 184–188
19 Livak, K. J., Schmittgen, T. D. (2001) Analysis of relative gene expression data using real-time quantitative PCR and the 2(-Delta Delta C(T)) Method. Methods 25, 402–408
20 Benvenuti, S., Saccardi, R., Luciani, P., Urbani, S., Deledda, C., Cellai, I., Francini, F., Squecco, R., Rosati, F., Danza, G., Gelmini, S., Greeve, I., Rossi, M., Maggi, R., Serio, M., Peri, A. (2006) Neuronal differentiation of human mesenchymal stem cells: changes in the expression of the Alzheimer's disease-related gene seladin-1. Exp. Cell Res. 312, 2592–2604
21 Formigli, L., Meacci, E., Sassoli, C., Squecco, R., Nosi, D., Chellini, F., Naro, F., Francini, F., Zecchi-Orlandini, S. (2007) Cytoskeleton/stretch-activated ion channel interaction regulates myogenic differentiation of skeletal myoblasts. J. Cell Physiol. 211, 296–306
22 Sartiani, L., Bettiol, E., Stillitano, F., Mugelli, A., Cerbai, E., Jaconi, M. E. (2007) Developmental changes in cardiomyocytes differentiated from human embryonic stem cells: a molecular and electrophysiological approach. Stem Cells 25, 1136–1144
23 Donati, C., Meacci, E., Nuti, F., Becciolini, L., Farnararo, M., Bruni, P. (2005) Sphingosine 1-phosphate regulates myogenic differentiation: a major role for S1P2 receptor. FASEB J. 19, 449–451
24 Inniss, K., Moore, H. (2006) Mediation of apoptosis and proliferation of human embryonic stem cells by sphingosine-1-phosphate. Stem Cells Dev. 15, 789–796
25 Kleger, A., Busch, T., Liebau, S., Prelle, K., Paschke, S., Beil, M., Rolletschek, A., Wobus, A., Wolf, E., Adler, G., Seufferlein, T. (2007) The bioactive lipid sphingosylphosphorylcholine

induces differentiation of mouse embryonic stem cells and human promyelocytic leukaemia cells. Cell Signal. 19, 367–377
26 Pebay, A., Wong, R. C. B., Pitson, S. M., Wolvetang, E. J., Peh, G. S. L., Filipczyk, A., Koh, K. L. L., Tellis, I., Nguyen, L. T. V., Pera, M. F. (2005) Essential roles of sphingosine-1-phosphate and platelet-derived growth factor in the maintenance of human embryonic stem cells. Stem Cells 23, 1541–1548
27 Donati, C., Cencetti, F., Nincheri, P., Bernacchioni, C., Brunelli, S., Clementi, E., Cossu, G., Bruni, P. (2007) Sphingosine 1-phosphate mediates proliferation and survival of mesoangioblasts. Stem Cells 25, 1713–1719
28 Annabi, B., Thibeault, S., Lee, Y. T., Bousquet-Gagnon, N., Eliopoulos, N., Barrette, S., Galipeau, J., Beliveau, R. (2003) Matrix metalloproteinase regulation of sphingosine-1-phosphate-induced angiogenic properties of bone marrow stromal cells. Exp. Hematol. 31, 640–649.
29 Donati, C., Bruni, P. (2006) Sphingosine 1-phosphate regulates cytoskeleton dynamics: implications in its biological response. Biochim Biophys Acta. 1758, 2037–2048
30 Benvenuti, S., Saccardi, R., Luciani, P., Urbani, S., Deledda, C., Cellai, I., Francini, F., Squecco, R., Rosati, F., Danza, G., Gelmini, S., Greeve, I., Rossi, M., Maggi, R., Serio, M., Peri, A. (2006) Neuronal differentiation of human mesenchymal stem cells: changes in the expression of the Alzheimer's disease-related gene seladin-1. Exp. Cell Res. 312, 2592–2604
31 Li, G. R., Sun, H., Deng, X., Lau, C. P. (2005) Characterization of ionic currents in human mesenchymal stem cells from bone marrow. Stem Cells 23, 371–382
32 Heubach, J. F., Graf, E. M., Leutheuser, J., Bock, M., Balana, B., Zahanich, I., Christ, T., Boxberger, S., Wettwer, E., Ravens, U. (2004) Electrophysiological properties of human mesenchymal stem cells. J. Physiol 554, 659–672
33 Crescioli C, Squecco R, Cosmi L, Sottili M, Gelmini S, Borgogni E, Sarchielli E, Scolletta S, Francini F, Annunziato F, Vannelli GB, Serio M. (2008) Immunosuppression in cardiac graft rejection: a human in vitro model to study the potential use of new immunomodulatory drugs. Exp. Cell Res. 314,1337–1350
34 Morelli, A., Squecco, R., Failli, P., Filippi, S., Vignozzi, L., Chavalmane, A. K., Fibbi, B., Mancina, R., Luciani, G., Gacci, M., Colli, E., Francini, F., Adorini, L., Maggi, M. (2008) The vitamin D receptor agonist elocalcitol upregulates L-type calcium channel activity in human and rat bladder. Am. J. Physiol. Cell Physiol. 294, C1206-C1214
35 Jeon, E. S., Moon, H. J., Lee, M. J., Song, H. Y., Kim, Y. M., Bae, Y. C., Jung, J. S., Kim, J. H. (2006) Sphingosylphosphorylcholine induces differentiation of human mesenchymal stem cells into smooth-muscle-like cells through a TGF-beta-dependent mechanism. J. Cell Sci. 119, 4994–5005
36 Jeon, E. S., Park, W. S., Lee, M. J., Kim, Y. M., Han, J., Kim, J. H. (2008) A Rho kinase/myocardin-related transcription factor-A-dependent mechanism underlies the sphingosylphosphorylcholine-induced differentiation of mesenchymal stem cells into contractile smooth muscle cells. Circ. Res. 103, 635–642
37 Pebay, A., Bonder, C. S., Pitson, S. M. (2007) Stem cell regulation by lysophospholipids. Prostaglandins Other Lipid Mediat. 84, 83–97
38 Avery, K., Avery, S., Shepherd, J., Heath, P. R., Moore, H. (2008) Sphingosine-1-phosphate mediates transcriptional regulation of key targets associated with survival, proliferation, and pluripotency in human embryonic stem cells. Stem Cells Dev. 17, 1195–1205
39 Sachinidis, A., Gissel, C., Nierhoff, D., Hippler-Altenburg, R., Sauer, H., Wartenberg, M., Hescheler, J. (2003) Identification of plateled-derived growth factor-BB as cardiogenesis-inducing factor in mouse embryonic stem cells under serum-free conditions. Cell Physiol. Biochem. 13, 423–429
40 Ishii, I., Fukushima, N., Ye, X., Chun, J. (2004) Lysophospholipid receptors: signaling and biology. Annu. Rev. Biochem. 73, 321–354
41 Means, C. K., Xiao, C. Y., Li, Z., Zhang, T., Omens, J. H., Ishii, I., Chun, J., Brown, J. H. (2007) Sphingosine 1-phosphate S1P2 and S1P3 receptor-mediated Akt activation protects against in vivo myocardial ischemia-reperfusion injury. Am. J. Physiol. Heart Circ. Physiol. 292, H2944-H2951
42 Gurevich, V. V., Gurevich, E. V. (2008) How and why do GPCRs dimerize? Trends Pharmacol. Sci. 29, 234–240
43 Schuppel, M., Kurschner, U., Kleuser, U., Schafer-Korting, M., Kleuser, B. (2008) Sphingosine 1-phosphate restrains insulin-mediated keratinocyte proliferation via inhibition of Akt through the S1P2 receptor subtype. J. Invest. Dermatol. 128, 1747–1756
44 Jeon, E. S., Kang, Y. J., Song, H. Y., Woo, J. S., Jung, J. S., Kim, Y. K., Kim, J. H. (2005) Role of MEK-ERK pathway in sphingosylphosphorylcholine-induced cell death in human adipose tissue-derived mesenchymal stem cells. Biochim. Biophys. Acta 1734, 25–33
45 An, S., Bleu, T., Huang, W., Hallmark, O. G., Coughlin, S. R., Goetzl, E. J. (1997) Identification of cDNAs encoding two G protein-coupled receptors for lysosphingolipids. FEBS Lett. 417, 279–282
46 Kinner, B., Zaleskas, J. M., Spector, M. (2002) Regulation of smooth muscle actin expression and contraction in adult human mesenchymal stem cells. Exp. Cell Res. 278, 72–83
47 Wang, D., Park, J. S., Chu, J. S., Krakowski, A., Luo, K., Chen, D. J., Li, S. (2004) Proteomic profiling of bone marrow mesenchymal stem cells upon transforming growth factor beta1 stimulation. J. Biol. Chem. 279, 43725–43734
48 Xin, C., Ren, S., Kleuser, B., Shabahang, S., Eberhardt, W., Radeke, H., Schafer-Korting, M., Pfeilschifter, J., Huwiler, A. (2004) Sphingosine 1-phosphate cross-activates the Smad signaling cascade and mimics transforming growth factor-beta-induced cell responses. J. Biol. Chem. 279, 35255–35262
49 Kono Y, Nishiuma T, Nishimura Y, Kotani Y, Okada T, Nakamura S, Yokoyama M. (2007) Sphingosine kinase 1 regulates differentiation of human and mouse lung fibroblasts mediated by TGF-beta1. Am. J. Respir. Cell Mol. Biol. 37, 395–404.
50 Donati, C., Cencetti, F., De Palma, C., Rapizzi, E., Brunelli, S., Cossu, G., Clementi, E., Bruni, P. (2009) TGFbeta protects mesoangioblasts from apoptosis via sphingosine kinase-1 regulation. Cell Signal.21, 228–236